Reports

Earth Tides, Global Heat Flow, and Tectonics

Abstract. *The power of a heat engine ignited by tidal energy can account for geologically reasonable rates of average magma production and sea floor spreading. These rates control similarity of heat flux over continents and oceans because of an inverse relationship between respective depth intervals for mass transfer and consequent distributions of radiogenic heat production.*

From the standpoint of material behavior, the earth tides could contribute significantly to tectonic processes (*1, 2*). Thus there is a possibility that heat and mass transfer in the earth's crust and upper mantle are influenced by tidal energy (*3, 4*).

The total heat flow from the earth's surface is about 3×10^{20} erg sec^{-1} (*5*), and tidal power is about 3×10^{19} erg sec^{-1} (*6*). Since two-thirds of the tidal energy is dissipated in the oceans, about 10^{19} erg sec^{-1} of tidal energy must be dissipated in the solid earth (*7*). Although at present tidal energy accounts for no more than 10 percent and probably only 3 percent of the average surface flux, it is strongly focused by dissipation mechanisms and can locally dominate other energy sources. Earth tides may act as a "catalytic agent"; that is, they may influence tendencies toward dynamic equilibrium in the earth. This role is possible even if the gross heat balance depends mainly on the distribution of radiogenic elements and secular cooling of the deep interior by large-scale convective heat transfer. By illustration, I first consider the total heat budget and then show how a global balance of shallow heat sources and surface flux could have evolved from tidal power in the form of melting and magmatic transfer. In this sense, tidal power has controlled the development of chemical gradients in the crust and upper mantle, and these gradients control the distribution of radiogenic heating. Because magmatic transfer also acts to focus larger-scale convection, the role of tidal energy in completing the heat balance is explained. Finally, compatible average chemical gradients beneath continents and oceans are deduced and are found to agree with current geophysical knowledge.

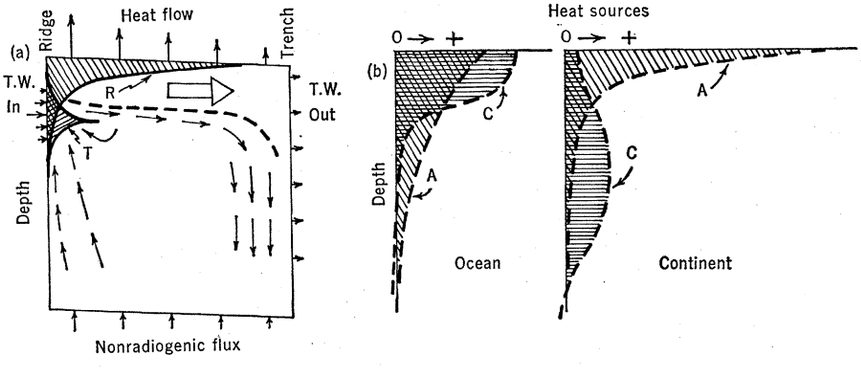

Fig. 1. Schematic model of heat cycle and distributions of heat sources near the earth's surface. (a) Vertical section across half-cell of an oceanic flow system. Cross-hatched areas indicate vertical (not lateral) distribution of radiogenic (R) and tidal (T) heat production near center of cell. The heavy dashed line marks the base of the spreading layer analogous to the model of Isacks *et al.* (*19*). Vectors indicate magnitudes of heat transfer across cell boundaries; *T.W.* is tidal work considered as a source term along ridge axis and a viscous loss across bounding shear zones in vicinity of the trench; flow trajectories imply only a general source-sink balance, not laminar cellular convection. (b) Schematic balance of principal heat transfer components between average continental and oceanic sections: A, radiogenic source distribution (not to same scale as Fig. 1a); C, convective source distribution. The convective source is relative to distributions of heat content in models of steady-state conduction; negative values are required at greater depths because of conservation of mass. The surface intercepts of C depend on average rates of volcanism. Nearly constant surface flux is obtained if the sum of the shaded areas is about the same in each section; Table 1 suggests that the areas under each of the curves are similar.

The similarity in average heat flux over continental and oceanic areas suggests either an unlikely coincidence of transient heat transfer mechanisms or a quasi-steady balance of integrated source terms over average continental and oceanic sections of the crust and upper mantle (see *3–5, 8*). In continental provinces Roy *et al.* (*9*) have found that the surface flux is given by

$$q = q_0 + DA_s \qquad (1)$$

where q_0 is a deep flux (roughly constant within a province) and A_s is the local rate of surface heat production by radioactive decay considered constant in the depth interval D. The term DA_s is assumed here to represent the total radiogenic source q_{rad} along a given earth radius. Lachenbruch (*10*) points out that the same balance is obtained if the heat source decreases exponentially with depth:

$$A = A_s \exp(-Z/D_\delta) \qquad (2)$$

where A is the local rate of heat production at depth Z, A_s is the rate at the earth's surface, and D_δ is the logarithmic decrement of the heat source distribution with depth. The integrated radiogenic contribution to the surface flux is

$$q_{\text{rad}} = A_s D_\delta [1 - \exp(-Z/D_\delta)] \qquad (3)$$

which gives the total contribution as $q_{\text{rad}} = A_s D_\delta$. Geologically, Eq. 2 represents a continuous approximation to finite intervals and expresses a gross compositional stratification in the continents. In the Sierra Nevada, D_δ is about 10 km (*10*), and a range of 7 to 10 km is characteristic of many other North American localities (*9*). The term q_0 is taken to represent heat flux from the mantle; values in North America range from about 15 to 60 erg cm^{-2} sec^{-1} (*9, 10*).

If average heat flux from the ocean basins is nearly the same as the continental flux, then there is a balance:

$$\begin{matrix} q' = q \\ D'A'_s = D_\delta A_s - \Delta q_0 \end{matrix} \qquad (4)$$

where primed quantities refer to the oceans, unprimed quantities refer to the continents, $\Delta q_0 = (q'_0 - q_0)$ and D' is an *apparent* oceanic source interval; that is, it is simply a length which, multiplied by the surface heat production, gives the total radiogenic contribution. The subscript δ is used to signify

a length as a logarithmic decrement; values of D or D' without subscripts refer to characteristic depth intervals where the form of the source gradient is not specified.

There are two interesting limits of Eq. 4:

(i) $\Delta q_0 \to 0$; $D' A_s' \sim D_\delta A_s$

(ii) $\Delta q_0 \to D_\delta A_s$; $D' A_s' \sim 0$

The first limit corresponds to equality of integrated radiogenic sources between average oceanic and continental sections, and the second limit corresponds to concentration of all the earth's radioactive heat production in the continents.

The magnitude of an apparent source interval, D or D', for broad geographic regions can be guessed from the ranges of heat flow values and ranges of radioactive heat production in surface rocks. For example, in the Sierra Nevada province (*10*) the range of heat flow values is about 20 to 55 erg cm^{-2} sec^{-1} and surface heat production ranges from about 4×10^{-6} to 40×10^{-6} erg cm^{-3} sec^{-1}, which gives the ratio $D = \Delta q / \Delta A_s = 10$ km, as found above (*9*, *10*). In oceanic regions, the ranges of q' are similar to ranges of q, but the ranges of A_s' are usually smaller than ranges of A_s, from nearly zero to about 5×10^{-6} erg cm^{-3} sec^{-1} (*11*), suggesting $D' \sim 80$ km, with a large uncertainty.

However, a constraint is placed on the oceanic heat balance by models of sea floor spreading. Sleep (*12*) computed the heat flow for a spreading model that was compatible with gravity anomalies and topography across oceanic ridges. By assuming a spreading layer with a thickness of 100 km and a total length of ridges of 6×10^4 km, he found that an average spreading rate of 2 cm yr^{-1} accounts for about 1×10^{20} erg sec^{-1}, or about half of the total oceanic heat flow. This component of heat flow is viewed here as a short circuit of the deep heat flux to regions nearer the surface by upward mass transfer in the vicinities of oceanic ridges. By this interpretation, $q_0' \sim q'_{\text{rad}}$ on the average.

The heat balances outlined above (see Table 1 and Fig. 1) suggest that $\Delta q_0 \sim 0$, and the nonradiogenic flux is roughly half the total flux in both continents and ocean basins. If a smaller average value of A_s were used, such as the average for the Canadian shield (*13*), the average nonradiogenic flux into the continents would be much larger. If the nonradiogenic flux into the oceans is attributed to mass transfer,

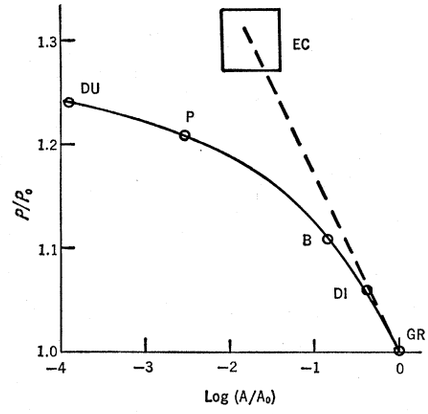

Fig. 2. Reduced density, $\phi = \rho/\rho_0$, versus reduced heat production, $\xi = A/A_0$, of average rock types for $\rho_0 = 2.67$ g cm^{-3}, $A_0 = 30 \times 10^{-6}$ erg cm^{-3} sec^{-1} (*4*, *22*); *GR*, granite; *DI*, diorite; *B*, basalt; *P*, peridotite; *DU*, dunite; *EC*, eclogite. The dashed line is given by Eq. 6.

then the magnitude of the deep continental flux requires similar mass transfer or much larger thermal conductivities; otherwise it is difficult to reconcile the fluxes with other constraints on thermal gradients discussed by Clark and Ringwood (*14*).

The heat balances suggest an inverse relationship: globally similar mass transfer is radially concentrated at higher levels beneath the oceans; globally similar radiogenic heat production is radially concentrated at higher levels in the continents (see Fig. 1b). This quasi-steady state maintains the correct distribution of mass demanded by measurements of the external gravity field and maintains, on the average, a constant radial composition per unit area (*15*). I will return to the significance of D' viewed as a logarithmic decrement D_δ'.

Although the dissipative source of heat contributed by the earth tides is small compared with heat flow, it can be important in the form of magma production influencing mass transfer. The rate of magma production equivalent to tidal power of 10^{19} erg sec^{-1} is about 30 km^3 yr^{-1}, based on a latent heat of 1×10^{10} erg cm^{-3} (about 100 cal g^{-1}). Specific heat is not included because the gross heat balance implies that thermal gradients approach the melting curve (*14*). If the magmatic injection component of sea floor spreading initiates at depths shallower than the interval considered by Sleep (*12*), then the possible tidal magma production alone can account for much of the average spreading rate (for instance, with a depth of 30 km and a total length of 6×10^4 km, the spreading rate by injection averages about 1 cm yr^{-1}, if a relatively small extrusion rate of lava is assumed). Magmatic injection along ridges transfers heat both from the tidal source and from stored heat in the mantle. Consequently, a compensating mass transfer from deeper regions is required to maintain the quasi-steady state. Thus, a tidal-magmatic mechanism can act as a trigger to the convective circulation (Fig. 1). Cyclical tidal strains along ridge axes may maintain magmatic access to the surface and may also concentrate the energy dissipation.

The proposed mechanism by which tidal energy is converted to magma production is a form of shear melting (*1*). Kê's mechanism of viscous dissipation in polycrystalline materials (*16*) suggests that shear melting (*1*) is plausible at the tidal frequency, as follows. A dissipation quotient, Q^{-1}, is given by

$$Q^{-1} = 1/2\pi \cdot (\Delta E/E) \qquad (5)$$

where $\Delta E/E$ is the proportion of energy dissipated to maximum strain energy stored during a deformation cycle. Zener (*17*) shows that in cyclical defor-

Table 1. Approximate averages of heat flow parameters used in this report. Proportioning is based on a total heat flow of 3×10^{20} erg sec^{-1} (*5*). Italicized values are based on heat flow estimates compatible with sea floor spreading (*12*). q is average flux, where surface areas are based on a total of 5.1×10^{18} cm^2 and a ratio of ocean basins to continents of 2 : 1. A_s is surface heat production (see *11*). D_δ is the logarithmic decrement of the radiogenic source distribution; the oceanic value of 80 km corresponds to $\Delta q = 40$ erg cm^{-2} sec^{-1} and a heat production range from "submarine tholeiites" to "alkalic basalts" (see *11*), and the oceanic value of 50 km is computed from sea floor spreading and the surface production of alkalic basalt. q_{rad} (which is equal to $A_s D_\delta$) is the radiogenic flux, taken to be the product of surface heat production and the apparent logarithmic decrement of the radiogenic source distribution. q_0 is the mantle flux; the first two entries are based on Eq. 1, and the italicized value is independently estimated from computations by Sleep (*12*). This value fixes the radiogenic flux, but the logarithmic decrement varies according to the assumed limits for surface heat production.

Source	q (erg cm^{-2} sec^{-1})	A_s (erg cm^{-3} sec^{-1})	D_δ (km)	q_{rad} (erg cm^{-3} sec^{-1})	q_0 (erg cm^{-2} sec^{-1})
Continent	60	30×10^{-6}	10	30	30
Ocean	60	5×10^{-6}	80	40	20
			50	*25*	*35*

mations Q^{-1} is maximized at a value $\omega\tau = 1$, where ω is the angular frequency (1.41×10^{-4} sec^{-1} for the semidiurnal tide) and τ is a relaxation time (7.1×10^{3} sec for a dissipation peak at the tidal frequency). The relaxation time can be translated to an apparent viscosity from the Maxwell relation $\tau = \eta_A/M$, where M is an "instantaneous" modulus of rigidity taken to be about 3×10^{11} dyne cm^{-2} (*18*), giving $\eta_A \sim 2 \times 10^{15}$ poises. Estimates of viscosity (*1*) suggest that dissipation is maximized in a partly molten region with a liquid fraction of 10 to 30 percent. Therefore, it seems likely that melting provides the mechanism for dissipating a major fraction of tidal energy in the asthenosphere. Since this mechanism also regulates the amount of melting for peak dissipation, it may be an important control on uniformity of magmatic compositions.

The contribution of tidal energy to sea floor spreading should be roughly comparable to viscous dissipation below the rigid spreading layer, because conservation of energy in a steady-state system requires that the power of a "tidal pump" must be balanced by an equivalent friction loss in the flow (Fig. 1a). The viscous dissipation rate is the product of shear stress and shear rate $\sigma\dot{\epsilon}$, or $\eta\dot{\epsilon}^2$, if η is a Newtonian viscosity (*1*). An interval of 100 km for the vertical velocity gradient in the asthenosphere (*19*) and an average spreading rate of 2 cm yr^{-1} gives an average shear rate of 7×10^{-15} sec^{-1}. The uplift calculated by Sleep (*12*) gives a measure of the lateral gradient and a shear stress of about 10^{8} dyne cm^{-2} in the asthenosphere. The corresponding dissipation rate is 7×10^{-7} erg cm^{-3} sec^{-1}, or 3×10^{-7} erg cm^{-3} sec^{-1} for a Newtonian viscosity of 5×10^{21} poises (*20*). These local averages integrated over a 100-km asthenosphere give total dissipation rates of 3.5×10^{19} erg sec^{-1} and 1.5×10^{19} erg sec^{-1} which are in adequate agreement with tidal power. The viscous losses also tend to distribute shear melting beneath the spreading layer and across bounding shear zones (Fig. 1a).

As a first approximation, it is assumed that magmatic transfers of tidal origin affect oceanic and continental regions in proportion to their areas. In the continents, however, magmatic increments crystallizing deep in the crust transfer heat to compositions with lower solidus temperatures that are at shallower depths in the crust. The result is a form of zone melting that concentrates the most differentiated (radiogenically "hottest") and least dense fractions near the surface. In the steady state, the rate at which differentiated compositions build up balances the rate at which new magma enters the crust. The heat available to melt compositions higher in the crust is given roughly by latent heats of crystallization and heat capacities integrated over the differences in melting temperatures. Therefore, the volumetric rate of stratification should be somewhat greater than the rate of magma introduction. A rate that is one-third the possible tidal magma production gives 10 km^3 yr^{-1}, or 5×10^{-3} cm yr^{-1} averaged vertically over the total continental area. A 10-km layer of granitic composition could form in 200 million years, and the entire continental crust could have formed since the late Precambrian. The growth rate is more than adequate even without higher dissipation rates in the past (*6*), but it resembles rates of crustal evolution in western North America since the Mesozoic.

The tidal-magmatic model suggests that gradients of composition near the earth's surface may have evolved at rates proportional to dissipation of tidal energy. If rocks of various compositions and densities have been produced in similar volumes by magmatic processes and if the density distribution tends toward stability, then density is proportional to depth in the upper part of the "refined" zone in the crust and upper mantle; that is, density layers are distributed somewhat like a complex pousse-café (*21*). Therefore, if there were a systematic relationship between density, composition, and radiogenic heat production, the tidal mechanism of magma production could be linked to the gradients of radiogenic sources. A simple relationship would exist—for example, if Eq. 2 represented the radiogenic gradient and if the local radiogenic concentration were also an exponential function of density.

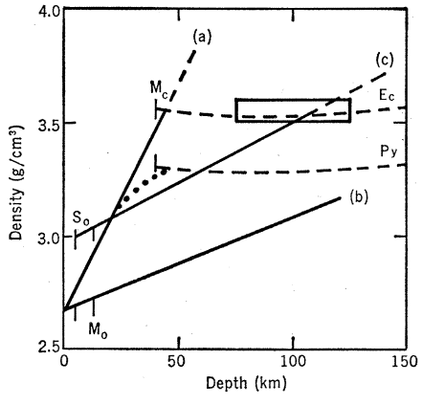

Fig. 3. Density versus depth predicted from correlation of radioactive source gradients (Eq. 2) with source density function (Eq. 6); (*a*) continental section for $D_\delta = 10$ km; (*b*) oceanic section for $D_\delta' = 50$ km; (*c*) oceanic section adjusted to $\rho_0' = 3.0$ g cm^{-3}, $A_0' = 5 \times 10^{-6}$ erg cm^{-3} sec^{-1}, $D_\delta' = 50$ km. Curves *Ec* and *Py* are average eclogite and pyrolite models, respectively, of Clark and Ringwood (*14*). The box represents the independent determination by Press (*23*). The dotted curve is a trend analogous to the solid curve in Fig. 2. Zero depth is at the average continent surface; S_0 is average ocean floor; M_0 and M_c are approximate depths of respective seismic Mohorovicic discontinuities.

Figure 2 tests the relationship of average density to the logarithm of average heat production for typical rocks expressed in nondimensional units $\phi = \rho/\rho_0$ and $\xi = A/A_0$, where ρ_0 and A_0 are average values of density and heat production of granitic rocks taken as characteristic values near the continental surface. [For averages of A, see (*4*); for average densities, see (*22*).] The dashed line describes the function

$$\xi = \exp[13.4\,(1 - \phi)] \qquad (6)$$

which satisfies the idealized gradients of density and heat production. That is, if A_0 represents a characteristic limit for A_s in Eq. 2, then density according to Eq. 6 is proportional to depth

$$\phi = 1 + (Z/13.4D_\delta) \qquad (7)$$

Thermal expansion and compressibility were ignored, but, if ρ_0 is also adjusted for P and T, the values of ϕ will be similar because of compensating changes.

The dashed line in Fig. 2 is interesting for the following reasons: (i) it approximates the solid curve for compositions characteristic of continental crust; (ii) it projects to values for eclogitic rocks that may be present in the suboceanic mantle (*23*); and (iii) it predicts reasonable values of density versus depth for an exponential distribution of radiogenic heat sources. Ostensibly, the dashed line could be satisfied by magmatic mineral assemblages ranging between granitic and eclogitic compositions. If so, the solid line represents some average trend of residual compositions rather than representative magmatic compositions.

Figure 3 gives density gradients from Eq. 7. Curve a represents the "observed" value $D_\delta = 10$ km. Curve b is an oceanic gradient computed as though the surface composition could attain the continental value at a hypo-

thetically comparable level. Curve c is the oceanic gradient normalized to a basaltic surface composition and density ($\rho_0' = 3.0$ g cm^{-3}, $A_0' = 5 \times 10^{-6}$ erg cm^{-3} sec^{-1})

$$\phi' = 1 + (Z'/13.4D_\delta') \qquad (7a)$$

where the oceanic source interval D' is interpreted as a logarithmic decrement, $D_\delta' = 50$ km. Curve c, based on D_δ' deduced from sea floor spreading, predicts the preferred density at 100 km computed by Press (*23*) for the suboceanic mantle. Curve a, however, does not discriminate between "pyrolite" and "eclogite" models, because the interval to 30 km ($3D_\delta$) contributes 95 percent of the total radioactive heat production. That is, the dotted curve in Fig. 3 could correspond to residual compositions like the solid curve in Fig. 2.

If the pyrolite model (*14*) were used to represent the continental subcrust to a depth of isostatic compensation near 400 km, apparently there would be a large mass excess beneath the oceans. The existing mass balance and the differences in surface elevations can be reconciled, however, if there is a pyrolite-type residue beneath the continents amounting to about 20 percent of this interval, or roughly 100 km. This thickness of residuum is compatible with the density distribution and heat production, and also with a granitic surface layer representing only a few percent of the original volume.

The present model of crust-mantle evolution describes a comparatively stagnant stratification in the continental crust relative to a "stirred" stratification in the oceanic subcrust. The contrast in density gradients fits the observation that a radiogenic source gradient between "basalt" and "eclogite" beneath the oceans is nearly an extension of a gradient between "granite" and "basalt" in the continents (Fig. 2). Although "eclogite" could satisfy the initial radiogenic compositions beneath continents and oceans, another common parental composition is possible.

In summary, magmatic processes triggered by tidal energy sources can provide the "working fluid" in a geodynamo operating as a coupled thermomechanical-thermochemical heat engine. Globally constant heat flux is consistent with equality of heat fluxes due to mass transfer and radioactive heat production in both continental and oceanic sections. The steady state is explained by an inverse relationship between the respective depth intervals for the two heat terms beneath continents and oceans. These intervals are related by magmatic transfers that simultaneously satisfy tidal energy, concentration of radioactive elements at continental surfaces, and sea floor spreading in the oceans. The resulting chemical gradients are consistent with heat flow and density gradients in the crust and upper mantle. The average heat flux, surface elevations, and gravity are nearly indifferent to "continental drift" relative to a depth where the chemical gradients beneath continents and oceans are similar; this depth is approximately $3D_\delta'$ (95 percent of q'_{rad}), or about 150 km by the present model.

HERBERT R. SHAW
U.S. Geological Survey,
Washington, D.C. 20242

References and Notes

1. H. R. Shaw, *J. Petrology* **10**, 510 (1969).
2. I. J. Gruntfest and H. R. Shaw, *Trans. Amer. Geophys. Union* **50**, 318 (1969).
3. See also data and references in *The Earth's Crust and Upper Mantle*, P. J. Hart, Ed. (American Geophysical Union, Washington, D.C., 1969); T. F. Gaskell, *The Earth's Mantle* (Academic Press, New York, 1967); P. J. Melchior, *The Earth Tides* (Pergamon, New York, 1966).
4. W. M. Kaula, *An Introduction to Planetary Physics* (Wiley, New York, 1969).
5. W. H. K. Lee and S. Uyeda, in *Terrestrial Heat Flow*, W. H. K. Lee, Ed. (American Geophysical Union, Washington, D.C., 1965), p. 87.
6. G. J. F. MacDonald, *Rev. Geophys.* **2**, 467 (1964); W. M. Kaula, *ibid.*, p. 661.
7. G. Miller, *J. Geophys. Res.* **71**, 2485 (1966).
8. See contour map in M. N. Toksöz, J. Arkani-Hamed, C. A. Knight, *ibid.* **74**, 3751 (1969). A "quasi-steady balance" refers to effects (as currently observed) of globally averaged processes active in the outer few hundred kilometers of the earth over times longer than 10^8 years. The range of possible time constants for heat transfer in the earth do not permit an unambiguous distinction between steady and unsteady states; compare R. D. Schuiling, *Nature* **210**, 1027 (1966).
9. R. F. Roy, D. D. Blackwell, E. R. Decker, F. Birch (abstract), *Trans. Amer. Geophys. Union* **49**, 319 (1968); R. F. Roy, D. D. Blackwell, F. Birch, *Earth Planet. Sci. Lett.* **5**, 1 (1968).
10. A. H. Lachenbruch, *J. Geophys. Res.* **73**, 6977 (1968).
11. M. Tatsumoto, C. E. Hedge, A. E. J. Engel, *Science* **150**, 886 (1965). Data were converted by using factors from F. Birch, in *Nuclear Geology*, H. Faul, Ed. (Wiley, New York, 1954), p. 148. The values for "granite" and "alkalic basalt" are used in this report for average limits of surface heat production in continents and oceans, respectively.
12. N. H. Sleep, *J. Geophys. Res.* **74**, 542 (1969); see also D. P. McKenzie, *ibid.* **72**, 6261 (1967).
13. D. M. Shaw, *Geochim. Cosmochim. Acta* **31**, 1111 (1967).
14. S. P. Clark, Jr., and A. E. Ringwood, *Rev. Geophys.* **2**, 35 (1964).
15. G. J. F. MacDonald, *ibid.* **1**, 587 (1963).
16. T.-S. Kê, *Phys. Rev.* **71**, 533 (1947).
17. C. Zener, *Elasticity and Anelasticity of Metals* (Univ. of Chicago Press, Chicago, 1948).
18. C. R. Kurkjian, *Phys. Chem. Glasses* **4**, 128 (1963).
19. B. Isacks, J. Oliver, L. R. Sykes, *J. Geophys. Res.* **73**, 5855 (1968); L. Knopoff, *Science* **163**, 1277 (1969).
20. R. K. McConnell, Jr., *J. Geophys. Res.* **70**, 5171 (1965).
21. L. Cotton, *Official Bartenders Guide* (Mr. Boston Distillers, Boston, 1965), p. 77.
22. *Handbook of Physical Constants*, S. P. Clark, Ed. (Geological Society of America, New York, rev. ed., 1966). The value for diabase was used for basalt and the range for eclogite is extended to the value recommended by S. P. Clark, Jr., and A. E. Ringwood [*Rev. Geophys.* **2**, 35 (1964)]. Figure 2 produced in detail would show various families of curves; see R. I. Tilling and D. Gottfried, *U.S. Geol. Surv. Prof. Pap. 614-E* (1969).
23. F. Press, *Science* **165**, 174 (1969).
24. I thank R. I. Tilling for discussions of radioactive heat production in rocks, and R. I. Tilling, E. C. Robertson, P. Toulmin, and P. B. Barton for reviews. I was strongly influenced by the important discoveries of R. F. Roy *et al.* and A. H. Lachenbruch, and by the contributions of N. H. Sleep and F. Press.

31 December 1969; revised 13 March 1970 ■

Exposed Guyot from the Afar Rift, Ethiopia

Abstract. *A series of originally submarine volcanoes has been found in the Afar Depression. Some of the volcanic structures are morphologically similar to oceanic guyots. One of them consists of strata of finely fragmented and pulverized basaltic glass. The fragmentation of the lava is probably the result of stream explosions taking place during the submarine eruption. The flat top of this guyot is considered to be a constructional feature; by analogy, it is suggested that not all oceanic guyots are necessarily the result of wave truncation of former volcanic islands.*

Flat-topped seamounts, known as guyots, have been reported from several localities of the Pacific Ocean in the last 30 years (*1*). Their origin is commonly ascribed to wave truncation and subsidence of former volcanic islands (*1*). As far as we know, emerged guyots have not been reported from the geological record, with the exception of a small structure from the Mono Lake area in California (*2*). Thus, it may be of interest to describe a structure in the Afar (or Danakil) Region of eastern Ethiopia that resembles oceanic guyots. Afar is a tectonic depression located between the Ethiopian Plateau and the Red Sea, from which it is separated by the Danakil Alps (Fig. 1). It is a region of great geological interest because the Eastern African Rift, the Indian Ocean (Carlsberg) Rift, and the Red Sea Rift meet there. Northern Afar is partly at altitudes lower than sea level (minimum of −120 m); it was a marine basin up to late Pleistocene time, when its connection with the Red Sea in the area